

NEAR-EQUATORIAL CONVECTIVE REGIMES OVER THE INDIAN OCEAN AS REVEALED BY SYNERGISTIC ANALYSIS OF SATELLITE OBSERVATIONS*

GAD LEVY and ANDREW GEISS

NorthWest Research Associates, Seattle, WA 98052, USA

M. R. RAMESH KUMAR

National Institute of Oceanography, Dona Paula, Goa, India

We examine the organization and temporal evolution of deep convection in relation to the low level flow over the Indian Ocean by a synergistic analysis of several satellite datasets for wind, rainfall, Outgoing Longwave Radiation (OLR) and cloud liquid water. We show that during the active Indian monsoon season, symmetric instability is present and is directly linked to organized convection and the off-equatorial location of the InterTropical Convergence Zone (ITCZ). The inertial regime interacts with and is controlled by monsoon and cross-equatorial flow. We characterize the dominant regimes of deep convective organization and the possible ocean-atmosphere mechanisms that control them at different phases of the Indian Monsoon. Ongoing work on development of algorithms for automated identification of convective regimes in climate data and their application and testing on 30 years of OLR data are discussed, and preliminary results of the double ITCZ organization in climate data are presented.

1. Introduction

When averaged over time, tropical deep convection appears to organize into coherent structures. One notable tropical convective organization is along an east-west line known as the InterTropical Convergence Zone (ITCZ), often considered as the earth's meteorological equator.¹ Tropical organized deep convection forms in (and often marks) the upward branch of the Hadley circulation. Depending on longitude, season, meteorological regime, averaging scale, and the state of ENSO, the deep convective organization

*Work supported by grant ATM- 0741832 of the US National Science Foundation. Work supported by ISRO grant.

may appear more or less linear, sharp or fuzzy; its distance from the equator may vary, and on occasion a parallel, secondary line of convection forms.^{2,3} Reference 2 examines the climatological extent to which a second ITCZ opposite the equator forms (double ITCZ, or DITCZ) based on monthly precipitation distribution, and finds it to occur in the Indian Ocean (IO) primarily in November.

Several authors^{3,7-9} suggested that the circulation of the lower troposphere may be inertially unstable in regions where the isoline of absolute vorticity (AV) is displaced off the equator, and that such instability interacts with convection in the ITCZ. Such interactions would then determine the nature of convective organization in the tropics and how it regulates and feeds instabilities that originate directly and indirectly from the ITCZ. The latter include equatorially trapped and westward propagating waves emanating from ITCZ instability upstream, and intense Tropical Cyclones (TCs — hurricanes and typhoons) that they spawn.

Climate models generally do a poor job resolving the ITCZ and representing its structure correctly.^{10,11} This failure is “deleterious to an understanding of paleoclimate and predictions of future climate change”.¹² It is plausibly due to the misrepresentation of moist transient disturbances comprising the ITCZ. These disturbances have intricate horizontal and vertical structure and may be sensitive to the meridional gradient of potential vorticity on a very small meridional scale. It is likely that a misrepresentation of the Hadley circulation itself is equally to blame.

These issues are evidently important for determining the structure of the circulation, the latitude of the ITCZ, and possible double ITCZ. As an important step in resolving these issues and providing guidance to climate models, we present indisputable evidence from the IO and from global observations of surface wind that the isoline of zero AV is displaced off the equator, to varying degrees at different places and times. These displacements correlate well with the latitude of the ITCZ as measured by OLR. We also suggest that the intrusion of anomalous vorticity is deep at certain phases of the Indian monsoon and correlates well with the off-equatorial position of the ITCZ. We further present evidence of dominance or absence of convective organization along double line (DITCZ) at different phases of the Indian monsoon, and how it relates to symmetric stability of the low level flow. The closely related considerations of inertial stability and convective organization are evidently important to the dynamics in the tropical atmosphere, the locus of cloudiness and precipitation, and tropical storm tracks. A fairly precise knowledge of the organization of equatorial

deep convection is also needed for the purpose of the three-dimensional extratropical circulation and tropical air–sea interactions.

Developments in observational technology in recent decades have contributed significantly to our ability to observe remotely both convection and the low level flow in otherwise sparsely observed tropical oceanic regions, allowing us to diagnose the dynamics of convective organization with respect to the low level flow and its symmetry.

In this paper, we review recent and ongoing work that utilizes the advanced observational technology and examines the organization of near-equatorial deep convection. We present a synergistic analysis of several satellite datasets for wind, rainfall, Outgoing Longwave Radiation (OLR) and cloud liquid water that characterizes the dominant regimes of deep convective organization in IO and shows the occurrence of DITCZ in climate data at different phases of the Indian Monsoon.

We start by presenting a conceptual model of equatorial dynamics as they potentially relate to the monsoon, inertial regimes, cross-equatorial flow, the ITCZ and disturbances emanating from it. In Section 3, we present the data and methods used and reviewed, and in Section 4, we present observations of convective organization and dominant regimes in the IO from satellite observations. We conclude with a summary and some thought in Section 5.

2. Overview

Typically atmospheric deep convection in the tropics appears to organize along the ITCZ. It is tempting to regard the ITCZ as essentially a two-dimensional phenomenon owing to its horizontal anisotropy, but the role of the underlying ocean, monsoons, and 3D transients in forming the time-averaged structure is essential. Time-averaging brings the underlying ocean into play. On timescales longer than a couple of weeks, we begin to see coherent variations of deep convection and SST and the ocean responds to the tropical atmospheric variability. We can also see the forcing of upwelling and downwelling circulations associated with the tropical atmospheric processes.

Monsoon systems are among the most complex coupled atmospheric and oceanic weather and climate phenomena. They produce much of the rainfall in the tropics and their variability is notoriously difficult to predict at all temporal scales, from intra-seasonal to interdecadal. The energy released in these systems impacts the overall circulation in the tropics and influences the mid-latitudes through teleconnection patterns. Monsoons act

as strong modulators to deep tropical convective organization along the ITCZ and in the Hadley cell.

2.1. *Symmetric instability*

Combining the shallow water angular momentum equation, the thermodynamic energy equation, and the hydrostatic approximation, one can relate the angular momentum and the potential temperature through a thermal wind relation and create a second order diagnostic equation for the mean meridional stream function. A sufficient condition for the linear stability of a baroclinic vortex is that the stream function equation be elliptic throughout the domain. This requires that the discriminant (D) be non-negative. Furthermore, Ref. 4 showed that $D < 0$ anywhere in the domain is sufficient for instability and Refs. 5 and 6 showed that, on a sphere, the stability discriminant, D , is proportional to the potential vorticity (PV). The sign of D determines whether the mean flow is stable. Thus, for a statically stable barotropic (equatorial) atmosphere that we discuss here, the condition for symmetric instability reduces to the well-known condition for inertial instability,⁷

$$f(f + \xi) < 0 \quad (1)$$

where f is the earth vorticity, ξ is the vertical component of the relative vorticity and $\eta = (f + \xi)$ is the AV. The analysis presented here suggests that the circulation of the lower troposphere may be inertially unstable in regions where the isoline of absolute vorticity (AV) is displaced off the equator, and that such instability is driven by monsoon forcing, and feeds back into the primary Hadley circulation and results in secondary circulation.⁹

Figure 1 is a schematic conceptual model of the primary atmosphere–ocean interactions in the tropics and monsoon areas. The principal ITCZ is located on the summer side of the equator (right of midpoint). The local response of potential vorticity (PV) to the Hadley circulation attached to the principal ITCZ is manifest through convergence zones drawing cross-equatorial flow and a region of anomalous PV in the lower troposphere (LT) on the summer side of the equator, and another (more extensive but shallower) region of return flow and anomalous PV in the upper troposphere on the winter side. Reference 7 propose a positive feedback mechanism for the generation of anomalous PV, whereby the instability is continuously “fueled” by cross-equatorial flow. A secondary ITCZ may form on the winter side of the equator.³ The remote response of PV to deep convection in the summer hemisphere associated with (1) tropical cyclones or (2) monsoons

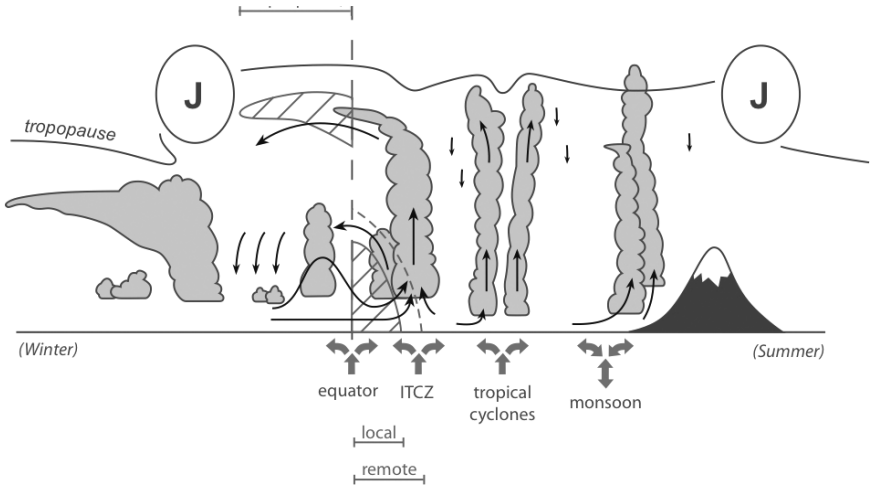


Fig. 1. A conceptual model of atmosphere–ocean interactions in the tropics.

(far from the equator in boreal summer) is to draw the region of anomalous PV farther from the equator compared to its nominal position. Figure 1 superposes the three primary forms of organized convection (ITCZ, TCs, and monsoons) although only one is usually dominant at a particular longitude and time. For example, monsoons are associated with continents, while TCs occur over ocean. An intense TC just poleward of ITCZ latitudes may draw the ITCZ itself poleward or obliterate it temporarily.

3. Data and Methods

The primary sources of data for the analyses presented here are surface wind observations from the SeaWinds instrument on the QuikSCAT satellite (QS hereafter), the Hamburg Ocean Atmosphere Parameters and Fluxes from Satellite (HOAPS III) dataset,¹⁴ and Outgoing Longwave Radiation (OLR) observation from the National Oceanic and Atmospheric Administration (NOAA) satellites.

3.1. Data sets

The QS wind vectors used for vorticity and divergence calculations are derived from radar backscatter from the ocean surface and are limited to one level only. They are available for 10 years (1999–2009) and are used to diagnose surface divergence, vorticity, and areas that are symmetrically

unstable using the criterion in Eq. (1) for the period 2000–2008. They are gridded and processed to remove polar orbiting sampling artifacts using a time–space interpolation algorithm^{15,16} as described in Ref. 3.

The HOPAS III is a satellite-based climatology of precipitation, turbulent heat fluxes and freshwater budget (evaporation minus precipitation) that includes also related atmospheric state variables over the global oceans. It contains daily, pentad and monthly means of sea surface temperature, specific humidity, wind speed, evaporation, rainfall, fresh water flux, integrated columnar water vapor and cloud liquid water for a period of more than 18 years (i.e. from 7 July 1987 to 31 December 2005). All variables are derived from SSM/I passive microwave radiometers, except for the SST, which is taken from AVHRR measurements. The dataset includes multi-satellite averages, and inter-sensor calibration. This data set is used to document DITCZ in the 18 years climatology during the November–December transition period.

Deep convection is inferred from radiance measurements at the top of the atmosphere (TOA) through OLR minima. Deep convective clouds have high, cold cloud tops that are associated with low (minimum) OLR values in the tropics.^{17,18} We use a 30-year time series of OLR observations to characterize the dominant deep convective regimes, correlate them to symmetric stability regimes for the analyzed QS period, and compare an 18 year climatological subset to the corresponding HOPAS III analysis. The OLR data are interpolated with a space–time interpolator,¹⁹ which is similar to Ref. 15 in its ability to trade time and space,^{20,21} except that it is applied to OLR.

3.2. Detection algorithm

We develop and apply a data-mining algorithm designed to detect linear features in images. The algorithm uses image recognition techniques via wavelet transform and multi-resolution analysis,^{22,23} in conjunction with a graph-based grouping algorithm. This process is calibrated using a heuristics based algorithm involving visual analysis of a training set of 300 random images.

The OLR data over the IO basin are examined through the detection algorithm in order to study inter-tropical convergence zone (ITCZ) anomalies. We examine the presence, location, and organization of minima in the data to detect and catalog manifestations of double lines of convection [(D)ITCZs]. The algorithm is applied to NOAA’s 30-year OLR data to generate a DITCZ index for this region.

4. Convective Organization

The ITCZ emerges as a quasi two-dimensional line in IO in OLR data at six days and that line sharpens at 10–14 days.³ In the tropical eastern Pacific,⁸ the ITCZ is in a highly transient state with variability occurring on 3–8 day time scales.⁸ Globally, the ITCZ appears as a coherent linear feature when averaged for 8–14 days.^{3,8,13} Subsequently, the analysis presented in the following subsections is based on HOPAS III pentad dataset and OLR observations and the QS-derived fields averaged over 10-day periods.

4.1. *Inertial and convective regimes*

Alternative attempts to explain the regional differences in ITCZ dynamics consider the inertial regime, the convective organization, the cross-equatorial flow (CEF) and pressure gradient, SST distribution, and, in IO, the phase of the monsoon.^{3,8,9,13} Using the convective organization as the major classification, we can define the following major regimes in IO:

1. Off-equatorial, well defined ITCZ in the summer hemisphere. This regime is associated with active monsoon forcing, strong CEF and pressure gradient, inertially unstable belt with zero-AV line 5° – 10° off the equator, and inertially unstable return flow aloft.
2. ITCZ, often diffuse, near geographical equator during transition periods (retreat of active monsoon). This regime is associated with weak pressure gradient, weak or no CEF, inertially stable atmosphere (zero-AV line within 2° of the equator.)
3. DITCZ straddling the equator. This regime, too, occurs during transition periods and is associated with weak pressure gradient, weak or no CEF, and inertially stable atmosphere.

Using the criterion in Eq. (1), the above regimes fall in two distinct inertial regimes. In the eastern Pacific, Ref. 9 identify the inertially unstable regime with strong pressure gradients, placing the zero AV line equatorward of the main ITCZ, and note the alignment of the ITCZ and convection with maxima in SST when the atmosphere is inertially stable. In all oceanic regions except for the central Pacific, a positive correlation between the location of the zero AV line and that of the main ITCZ poleward of it exists.¹³

Normal linear correlations between the time series of the latitude of the zero-AV line, maximum convergence, and minimum OLR are good statistical measures of the association between the inertial/symmetric instability and the

convective organization along the ITCZ. By inference, they are also indicators of regional (basin) differences and the role of monsoonal forcing. Figure 2 displays the latitudinal location of the zero-AV line, maximum convergence, and OLR minimum used for correlation calculations for IO (top panels), Atlantic basin (middle panels), and Pacific basin (bottom panel). All variables are longitudinally averaged over the basin:

- Indian ocean: between 50°E and 100°E .
- Atlantic basin: between 50°W and 10°E .
- Pacific basin: between 150°E and 80°W .

The time series are filtered with a Lanczos filter²⁴ at 3 months cut-off to remove the higher-frequency fluctuations, and the correlation calculations are repeated (Fig. 2, lower panel for each basin).

The normal linear correlation coefficients between the latitude of the zero-AV line and that of maximum convergence, the latitude of the zero-AV line and that of minimum OLR, and the line of maximum convergence and that of minimum OLR are tabulated for all basins in Table 1 along with the variance they explain. Lag correlations do not improve the coefficients, suggesting that the time scale of the processes that may explain the correlations is shorter than the 10-day averaging scale.

Figure 2 and the correlations exhibit a strong seasonal dependence in the location of all variables in all basins. However, they also show significant regional differences in ITCZ dynamics, inertial regimes, and the strong and complex monsoon forcing that dominates those in IO. In IO, the convective organization locations of OLR and divergence minima show considerably higher frequency variability than in other basins, and the intrusion of symmetric instability (the zero-AV line) is significantly deeper, reaching farther away from the equator. The strong statistical association between the zero-AV line and the ITCZ location can be explained through the dynamical positive feedback mechanism suggested by Ref. 7. For the Indian summer monsoon, significant monsoonal asymmetrical forcing initially causes cross-equatorial flow, which forms an unstable region north of the equator. The mean zonal flow becomes increasingly westerly toward the north. Northward advection ($v > 0$) of the low angular momentum air crossing the equator decelerates this westerly zonal flow.

At the same time, easterly momentum, advected across the equator is turned to the north by the Coriolis force, thus reinforcing the northward flow. This process reinforces the instability and the cross-equatorial low-level

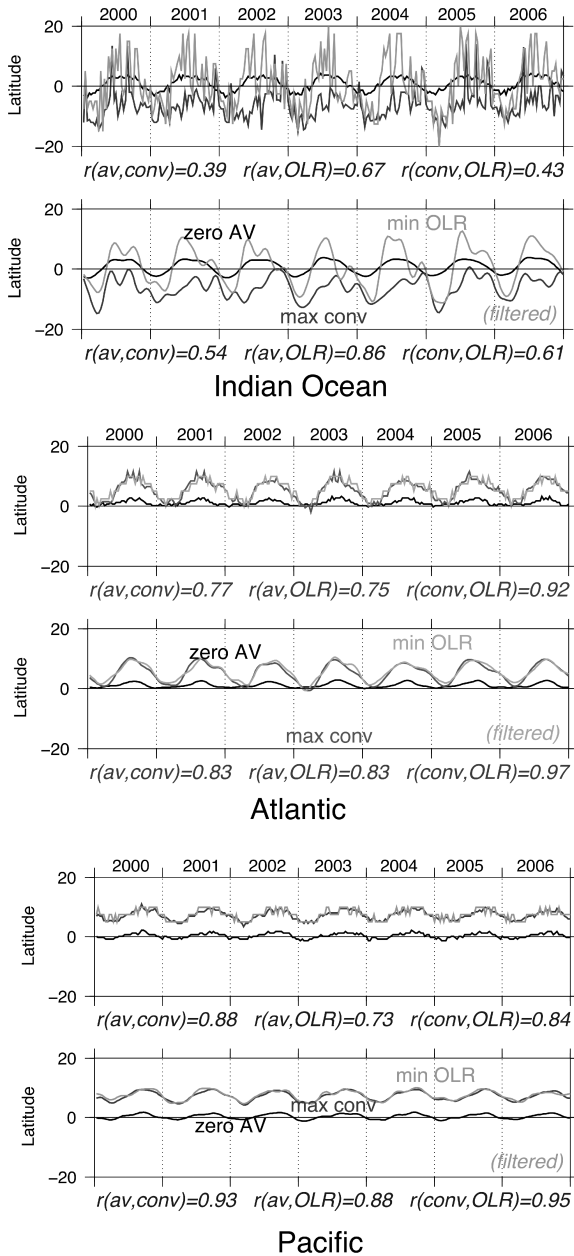


Fig. 2. Time-series of latitudinal location of the zero-AV line, maximum convergence, and OLR minima.

Table 1. Correlations between zero-AV line, maximum convergence, and OLR minima.

	0-AV line/Min OLR		0-AV line/Min divergence		Min OLR/Min divergence	
	No filter	Lanczos filter	No filter	Lanczos filter	No filter	Lanczos filter
Indian Ocean	0.67 (0.45) 44.9%	0.86 (0.74) 74%	0.39 (0.15) 15.2%	0.54 (0.29) 29.1%	0.43 (0.18) 18.5%	0.61 (0.37) 37.2%
Atlantic	0.77 (0.59) 59.3%	0.83 (0.69) 68.9%	0.75 (0.56) 56.2%	0.83 (0.69) 68.9%	0.92 (0.85) 84.6%	0.97 (0.94) 94.1%
Pacific	0.88 (0.77) 77.4%	0.93 (0.86) 86.5%	0.73 (0.53) 53.3%	0.88 (0.77) 77.4%	0.84 (0.70) 70.6%	0.95 (0.90) 90.2%

flow and gives rise to a secondary circulation due to inertial instability.⁹ The convergence produced by this secondary circulation determines the location of the maximum convection.^{3,7,9} A vertical (or slantwise) component to the motion caused by a 2D instability may drive the system back towards neutral stability by turbulent mixing of momentum. With sufficient lifting, a smaller westerly component is required for conservation of angular momentum, and the northward flow is further reinforced. This represents a positive feedback mechanism where the instability is continuously “fueled” by cross-equatorial flow.

4.2. Double ITCZs

Convective organization is very often misrepresented by global climate models,^{10,11} in particular when convection is organized bi-linearly.²⁵ As noted in the previous section, and by Ref. 3, such organization with DITCZ straddling the equator occurs in IO during transition periods. A weak signal of DITCZs over the IO in November was found in monthly mean precipitation data from Climate Prediction Centre Merged Analysis of Precipitation by Ref. 2. In this section, we preliminarily look at the occurrence of DITCZ in IO in climatological data. We first apply a detection algorithm to the 30-year OLR data to detect DITCZ occurrence for this region. We then examine the climate signal of DITCZ in November in the 18 year climatology covered in the HOAPS III dataset.

4.2.1. Double ITCZ index

The detection algorithm described in Section 3 is applied to all 30 years of OLR data available. To analyze the frequency of DITCZ presence, a DITCZ index (DI) is developed. The DI is based on four primary criteria:

1. The spatial extent of the DITCZ. A minimum length of 8 px is required. At a resolution of 2.5 deg/px, a DITCZ must extend zonally for 20°.
2. The linearity (in terms of R^2 (least square)) of the linear fit to the OLR minima in each individual convergence zone.
3. The degree to which the two convergence zones are parallel.
4. The degree to which the DITCZ has an East–West orientation.

Each criterion is weighted depending on its importance for defining a DITCZ, determined by applying a threshold value that minimized the number of discrepancies between the algorithm output and a manually evaluated randomly selected training set. In the index presented in Fig. 3, we use weights of 0.5, 0.25, 0.15, and 0.1 for criteria (1)–(4), respectively.

The DI is normalized on to a 0–1 scale. One represents a DITCZ that spans the full length of the image, has both convection bands perfectly parallel to the equator and to each other, and has perfectly linear convection bands. Zero represents the complete absence of a DITCZ. The DI therefore indicates both the presence and prominence of a DITCZ.

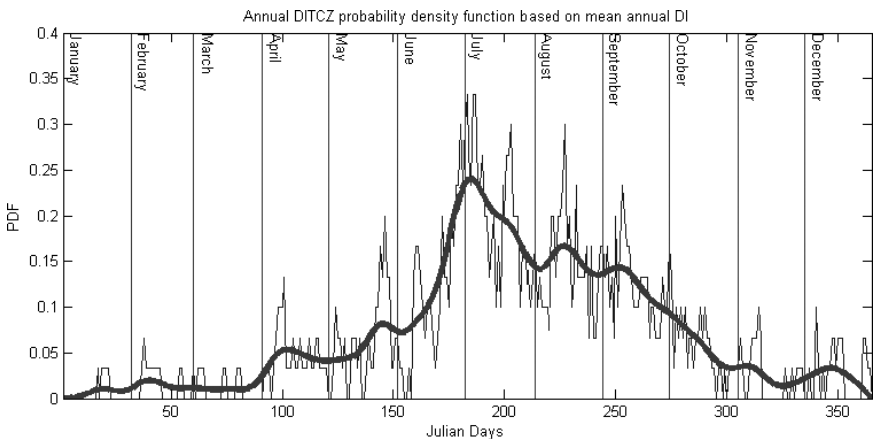


Fig. 3. Probability density function for average annual DITCZ presence based on 30-year OLR data set.

The DI was averaged over the 30-year data set resulting in the average annual signal of DITZ occurrence, shown in Fig. 3. It should be noted that our criteria for the DI are different than those of Ref. 2, and therefore cannot be used for direct comparison. For example, using the DI, we find that a DITCZ does not always straddle the equator. In some specific cases it can form with both convection bands on the same side of the equator, or one touching the equator.

4.2.2. Transition period double ITCZ

The results presented in Section 4.1 identify DITCZs straddling the equator during transition periods that are associated with inertially stable atmosphere³ and are also evident in Fig. 3. In monthly mean precipitation data, Ref. 2 found weak signals of Double ITCZs over the Indian Ocean in November. However, the temporal evolution of these in the Indian Ocean could not be ascertained, mainly because of the paucity of the data. A much stronger signal of the DITCZ emerges from synergistic analysis of rainfall and cloud liquid water from the HOAPS III data set and the corresponding 18-year climatology of OLR presented in Fig. 4.

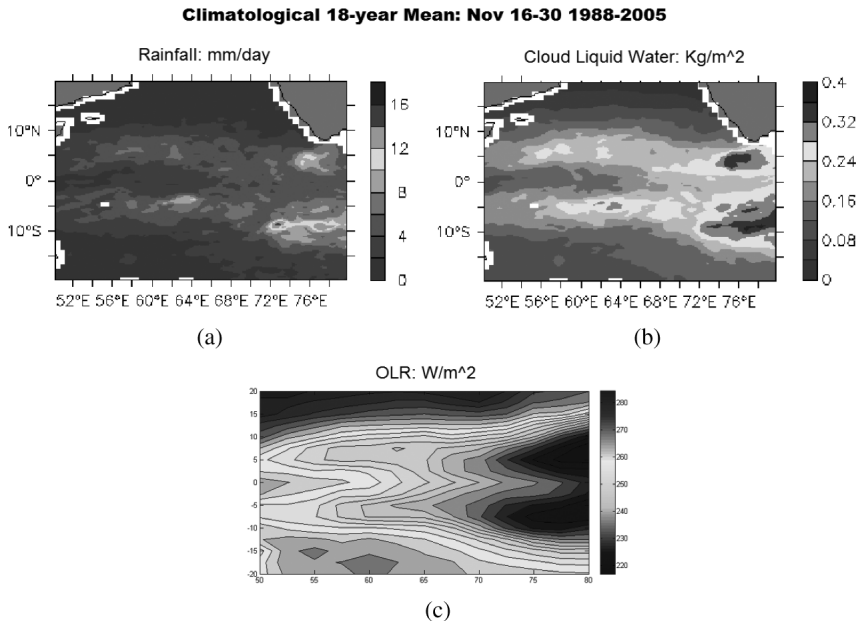


Fig. 4. Climatological mean distribution of (a) rainfall (mm/day) (b) cloud liquid water, and (c) OLR ($W m^{-2}$) showing double ITCZ structure over the western Indian Ocean during the Mature Phase (Nov. 16–30) for 1988–2005.

Figure 4 displays a climatological DITCZ during the last two weeks of November (November 16–November 30), when it is clearly visible in the composite images of the 18-year mean rainfall (4a), cloud liquid water (4b), and OLR (4c). At this “mature phase” of DITCZ lifecycle, both the branches are well established and well separated.²⁶

5. Summary and Conclusions

Examination of several satellite climate datasets over the Indian Ocean and other basins in recent and ongoing studies sheds some light and new findings about the organization of deep convection in monsoon areas. We show that during the active Indian monsoon season, symmetric instability is present and is directly linked to organized convection and the off-equatorial location of the ITCZ. The inertial regime interacts with and is controlled by monsoon, which draws cross-equatorial flow leading to significantly deeper intrusion of symmetric instability into the summer hemisphere. Deep convection along the ITCZ exhibits higher frequency variability in IO than in other basins — variability, which we attribute to monsoon forcing. We define three dominant regimes of deep convective organization, and characterize their dominance at different phases of the Indian Monsoon and the inertial regimes they correspond to. We offer physical and dynamic processes that can explain the statistical association we present. There are limitations to a statistical analysis’ ability to identify the various possible sources of a given dynamic variable or to partition it by physical source. Nonetheless, the correlations presented support statistically the physical and dynamical relationships and associations offered as explanations.

Ongoing work on algorithms for automated identification of convective regimes in climate data and its application to 30 years of OLR data reveals new, albeit preliminary, results on bi-linear convective organization and double ITCZ in this region.

Acknowledgments

This work was supported by the National Science Foundation under grant ATM-0741832. M. R. Ramesh Kumar was supported by an ISRO Grant.

References

1. D. E. Waliser and R. C. J. Somerville, *J. Atmos. Sci.* **51** (1994) 1619.
2. C. Zhang, *J. Geophys. Res.* **106** (2001) 11,785.
3. G. Levy and J. Patoux, *Int. J. Remote Sens.* **31** (2010) 4665.

4. K. Oomaya, *J. Atmos. Sci.* **23** (1966) 43–53.
5. B. J. Hoskins, *Quart. J. Roy. Meteor. Soc.* **100** (1974) 480–482.
6. D. E. Stevens, *J. Atmos. Sci.* **40** (1983) 882–893.
7. G. Levy and D. S. Battisti, *Glob. Atmos. Oce. Sys.* **3/4** (1995) 341.
8. R. A. Tomas and P. J. Webster, *Quart. J. Roy. Meteor. Soc.* **123** (1997) 1442.
9. V. E. Toma and P. J. Webster, *Clim Dyn.* (2009), doi: 10.1007/s00382-009-0584-x.
10. E. K. Vizy and K. H. Cook, *J. Geophys. Res.* **107** (2006) 10,1029.
11. A. Bellucci, S. Gualdi and A. Navarra, *J. Clim.* **23** (2010) 1127.
12. T. J. Dunkerton, *Bull. Amer. Meteorol. Soc.* **87** (2006) 1492.
13. G. Levy and T. J. Dunkerton, *GAYANA* **68** (2004) 420.
14. A. Andersson, S. Bakan, K. Fennig, H. Grassl, C.-P. Klepp and J. Schulz, doi: 10.1594/WDCC/HOAPS3_PENTAD.
15. L. Zeng and G. Levy, *J. Geophys. Res.* **100** (1995) 5133.
16. L. Zeng and G. Levy, *Advances in Space Research* **19** (1997) 537.
17. C. Lietzke, C. Deser and T. Haar, *Evolution, J. Clim.* **14** (2001) 743.
18. G. Magnusdottir and C. Wang, *J. Atmos. Sci.* **65** (2008) 2425.
19. B. Liebmann and C. A. Smith, *Bull. Amer. Meteor. Soc.* **77** (1996) 1275.
20. G. Levy and D. Vickers, *J. Geophys. Res.* **104** (1999) 20,639.
21. G. Levy, in *Remote Sensing of the Ocean and Sea Ice*, eds., C. R. Bostater Jr., R. Santoleri, 4172(SPIE), 1 (2000).
22. Y. Zhai and X. Liu, *IEEE: 6th World Congress on Intelligent Control and Automation*, 10289 (2006).
23. R. Strickland and H. Hahn, *IEEE Transactions on Image Processing* **6** (1997) 724.
24. C. E. Duchon, *J. Appl. Meteor.* **18** (1979) 1016.
25. L. F. Hubert, A. F. Kruger and J. S. Winston, *J. Atmos. Sci.* **26** (1969) 771.
26. M. R. Ramesh Kumar, A. Devasthale, G. Levy, S. Sankar, S. Bakan and H. Grassl, *Int. J. Remote Sens.* (in press, 2011).